Shear Thinning and Orientational Ordering of Wormlike Micelles

S. Förster,[1] M. Konrad,[1] and P. Lindner[2]
[1]*Institut für Physikalische Chemie, Universität Hamburg, D-20146 Hamburg, Germany*
[2]*Institut-Laue-Langevin, F-38042 Grenoble Cedex 9, France*
(Received 16 December 2003; published 13 January 2005)

Shear thinning and orientation of cylindrical surfactant and block copolymer micelles was investigated by rheo-SANS (small-angle neutron scattering) experiments. Shear thinning and orientation occur for shear rates $\dot{\gamma}\tau_{\mathrm{dis}} \gg 1$, where τ_{dis} is the disentanglement time of the micelles. Micelles align in the flow direction with an orientational distribution that can be well described by an Onsager-type distribution function. Over nearly the whole range of concentrations and for all cylindrical micelles investigated, the shear viscosity η follows a simple $\eta \sim e^{-aS}$ behavior as a function of the orientational order parameter S with the same prefactor a.

DOI: 10.1103/PhysRevLett.94.017803 PACS numbers: 61.25.Hq, 61.12.Ex

Amphiphilic molecules like surfactants and block copolymers can self-assemble into wormlike micelles [1]. These are interesting examples of linear chain structures for which linear polymers, carbon nanotubes, fibrous proteins, as well as inorganic and polymeric fibers, are further examples. Solutions of linear chain structures exhibit interesting rheological properties such as shear thinning and suppression of turbulant flow, which is related to flow-induced changes in chain conformation and orientation. These flow properties are of great relevance in technical applications as thickeners, drag reducers, and flow improvers, as well as in the production of fiber-reinforced materials.

A unique property of long chainlike molecules is the formation of entanglement networks. Already at low concentrations chain molecules start to overlap and entangle to form a transient network. Chainlike molecules subjected to a viscous shear gradient will orient in the flow, the instantaneous angular velocity being a function of the orientation relative to the local streamlines [2]. Below the overlap concentration $c < c*$, Brownian motion, characterized by a rotational diffusion coefficient, tends to randomize the orientations. The relative importance of the competing effects of shear orientation and Brownian motion is characterized by a dimensionless parameter $\Gamma = \dot{\gamma}\tau_{\mathrm{rot}}$ where $\dot{\gamma}$ is the shear rate and τ_{rot} the rotational diffusion time. Above the overlap concentration $c > c*$, rotational diffusion is constrained by entanglements, and the dynamical behavior is determined by $\Gamma = \dot{\gamma}\tau_{\mathrm{dis}}$, where τ_{dis} is the disentanglement time.

With increasing shear rate, chainlike molecules will orient leading to a decrease of the viscosity η (shear thinning). The degree of orientation can be described by the orientational order parameter $S = \langle(3\cos^2\delta - 1)/2\rangle$, which is related to a mean deviation angle $\langle\delta\rangle$ with respect to the flow direction. Theoretical predictions for the decrease of the viscosity with increasing order parameter have been given by Hayter and co-workers [3,4] and Doi [5] for rigid rodlike particles.

For wormlike micelles there have been few quantitative studies of the effect of increasing shear rate $\dot{\gamma}$ on shear vicosity η and orientational order parameter S. A quantitative relation of the bulk property η to a molecular property S enables a comparison to theoretical predictions by Hayter and Penfold [3] and Doi [5], and gives important insights into how shear affects flow and orientation of chainlike molecules. Well investigated model systems forming wormlike micelles are the surfactant systems cetyltrimethylammonium bromide (CTAB) and cetylpyridinium salicylate (CPySal) at different salt concentrations. Rheo-SANS (small-angle neutron scattering) studies on these systems showed that shear leads to highly anisotropic SANS patterns indicating shear orientation of cylindrical micelles [3,4,6,7]. Cylindrical micelles can also be formed by amphiphilic block copolymers [8]. Depending on block lengths, these micelles have cross-sectional diameters of 10–50 nm, which is considerably larger compared to CTAB and CPySal micelles with cross-sectional diameters of 4–5 nm. In this Letter we report the results of a comprehensive study of the effect of shear rate on the shear viscosity and orientational order parameter for cylindrical surfactant and block copolymer micelles of different thickness and concentration.

Three poly(butadiene-*b*-ethyleneoxide) (PB-PEO) block copolymers were synthesized by sequential living anionic polymerization of 1,3-butadiene and ethylene oxide in THF [9]. Degrees of polymerization were determined by matrix-assisted laser desorption/ionization–time of flight–mass spectrometer, gel permeation chromatography, and ^{1}H-NMR and are given in Table I. A fourth diblock copolymer, poly(ethylenebutylene-*b*-ethyleneoxide (PEB-PEO; TEGO from Goldschmidt), was lyophilized by freeze-drying from aqueous solution. Polydispersities for all block copolymers' samples are $M_w/M_n \leq 1.04$. CTAB,

TABLE I. Values for the degree of polymerization of the hydrophobic block, N_A, the hydrophilic block, N_B, the core radius, R_c, the overall cross-sectional radius, R_m, the density profile parameter, α, and the relative standard deviation of the cross-sectional radius, σ_R. Values for the surfactant system are also given when applicable.

Sample	N_A	N_B	R_c (nm)	R_m (nm)	α	σ_R
PB-PEO-14	147	204	13.5	20.5	0.54	0.13
PB-PEO-16	43	59	8.0	14.2	0.52	0.13
PB-PEO-17	27	51	6.0	11.5	0.54	0.13
PEB-PEO	39	102	9.8	21.2	0.55	0.12
CPySal		1	N.A.	2.1	0.00	0.15

cetylpyridinium bromide, and salicylic acid were purchased from Sigma and used as received. For rheo-SANS experiments the surfactants and block copolymers were dissolved in D_2O at concentrations of $c = 1\%$, 2%, 5%, and 10% w/w.

A Bohlin CVO stress-controlled rheometer was set up in the neutron beam at D11 (ILL, Grenoble). The quartz shear cell consisted of a stationary outer rotor and a rotating inner rotor (Searle geometry) with a 0.5 mm gap and was mounted in the radial and the tangential beam directions to probe the orientational distribution of the micelles in the flow-vorticity plane and in the gradient-vorticity plane, respectively. This setup allows one to cover a range of shear rates $\dot{\gamma} = 0.2$–$1000\ s^{-1}$. Data were collected on a 2D-^{3}He-filled area detector at a distance of 5.0 and 20.0 m. The neutron wavelength was $\lambda = 0.6$ nm with $\Delta\lambda/\lambda = 8\%$. Details of the instrumentation and data reduction can be found elsewhere [10].

Rheo-SANS experiments were performed such that the shear rates were increased stepwise from 0.2–$1000\ s^{-1}$. At each shear rate the shear viscosity η and the corresponding scattering pattern were recorded after an equilibration time of 1–2 min until the shear viscosity had reached a steady value. When subsequently reducing the shear rates from $1000 - 0.2\ s^{-1}$, the same viscosities and scattering patterns were accessed in reversed order, showing that the flow curves were completely reversible.

The structure and conformation of the micelles were determined by SANS in a dilute isotropic solution ($c = 2.0$ g/l). The scattering curves are shown in Fig. 1 together with fits (solid lines) to the form factor $P(q) = P_{||}(q)P_{\perp}(q)$ where $P_{||}(q)$ is the form factor of a Kratky-Porod wormlike chain [11] and $P_{\perp}(q)$ is the cross-sectional form factor for a cylindrical micelle with a homogeneous core and a shell with a $r^{-\alpha}$-density profile [12]. Such core-shell models have been shown to successfully describe the structure of block copolymer micelles [13]. The core and shell radii together with the exponent α are summarized in Table I. The persistence length determined from the Kratky-Porod chain model is $l_p \approx 100$ nm. In addition, the micellar structure was investigated by transmission electron microscopy (TEM) and atomic-force microscopy (AFM) [14]. TEM and AFM images show that micelles have contour lengths of up to several μm.

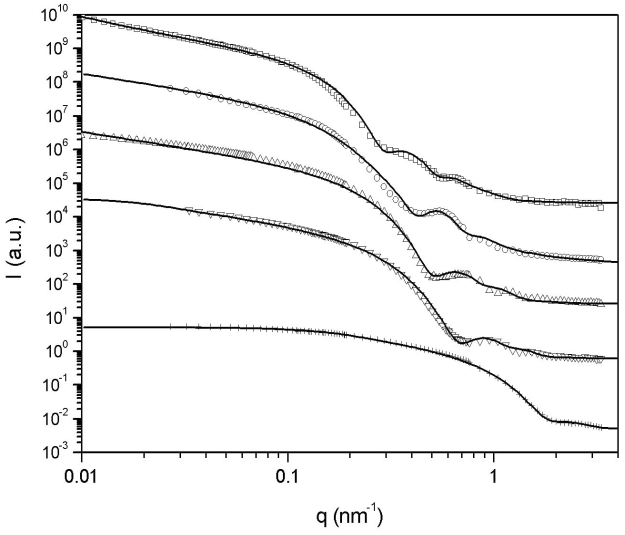

FIG. 1. Scattering curves of cylindrical micelles of PB-PEO-14 (□), PB-PEO-16 (○), PB-PEO-17 (△), PEB-PEO (▽), and CPySal (+) in D_2O. The curves are vertically offset for better visualization. The solid lines are fits to cylindrical micelles with core-shell cross sections.

Figure 2 shows the results of rheo-SANS experiments for wormlike micelles of PB-PEO-16, CPySal, and CTAB. All solutions show pronounced shear thinning where the

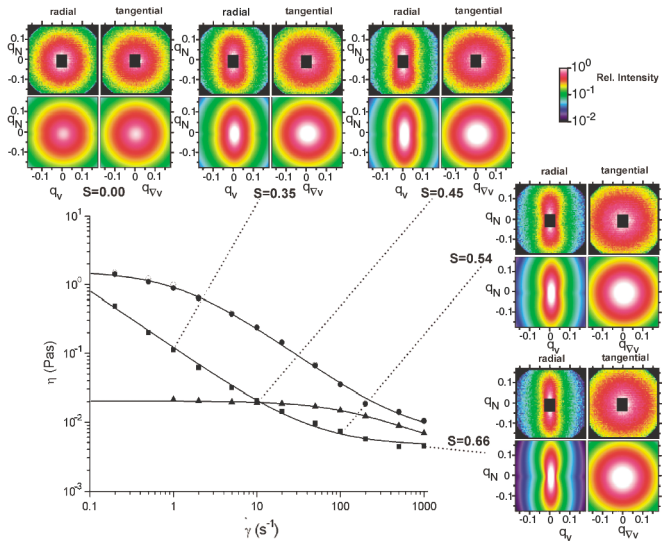

FIG. 2 (color). Shear viscosity η as a function of shear rate $\dot{\gamma}$ for cylindrical micelles at a concentration of $c = 20$ g/l: PB-PEO-16 (■), CPySal (●, ○), and CTAB (▲). Filled symbols are upward cycles, and open symbols are downward cycles. Measured (upper panels) and calculated (lower panels) SANS patterns are shown for PB-PEO-16 at rest (upper left) and at four different shear rates together with the calculated orientational order parameter S. The solid lines are fits to the Cross equation [Eq. (1)]. Scattering vectors in the flow direction q_v, gradient direction $q_{\nabla v}$, and vorticity direction q_N are given in nm^{-1}.

viscosity continuously decreases by more than 2 orders of magnitude with increasing shear rate. The shear-thinning behavior can well be described by the Cross equation

$$\frac{\eta - \eta_\infty}{\eta_0 - \eta_\infty} = \frac{1}{1 + (\tau_c \dot{\gamma})^n}, \quad (1)$$

where η_0 is the zero-shear viscosity, η_∞ the high-shear viscosity, τ_c the internal relaxation time, and n the power-law exponent characterizing the shear thinning between η_0 and η_∞. We observe n to decrease with increasing cylinder thickness from $n = 0.94$ for the thin surfactant micelles (CTAB, CPySal) to values down to $n = 0.60$ for thick block copolymer micelles (PB-PEO-14). Internal relaxation times as determined from Eq. (1) are $\tau_c = 4.5$ ms for CTAB and $\tau_c = 0.73$ s for CPySal. Most cylindrical block copolymer micelles have internal relaxation times of $\tau_c \gg 10$ s, so that τ_c and η_0 cannot be reliably determined in the available range of shear rates.

Figure 2 shows that with increasing shear rate the scattering patterns in the radial beam direction (flow-vorticity plane) become highly anisotropic, whereas the scattering patterns in the tangential beam direction (gradient-vorticity plane) stay isotropic. This is consistent with a flow-induced uniaxial orientation state of the cylindrical micelles in the shear direction, an assumption that is adopted in the following. In order to determine the orientational distribution of the cylinders, scattering patterns are calculated by

$$I(q_x, q_y) = \int_0^{\pi/2} \int_0^{2\pi} P(q, \beta(\delta, \chi)) h(\delta) d\chi d\delta, \quad (2)$$

where $h(\delta)$ is the fraction of cylinders with a deviation angle δ between cylinder axis and shear direction. The vectors describing the cylinder orientation are located on a cone having its central axis in the shear direction. The cylinder orientation is then completely determined by the rotation angle χ on the cone. From the angles (δ, χ) the angle β between cylinder axis and scattering vector can be calculated, which is necessary to compute the form factor $P(q, \beta)$ and the components (q_x, q_y) of the scattering vector [15]. As the orientational distribution function $h(\delta)$ is *a priori* not known, we investigated different functional forms including Boltzmann ($\exp[-(\delta/\bar{\delta})]$), Gaussian ($\exp[-(\delta/\bar{\delta})^2]$), Heaviside ($\Theta[\delta - \bar{\delta}]$), Maier-Saupe ($\exp[\cos^2(\delta/\bar{\delta})] - 1$), and Onsager ($\exp[-\sin(\delta/\bar{\delta})]$), as well as a generalized Laguerre function and a distribution function derived by Hayter and Penfold [3]. These distribution functions cover functional forms ranging from a step function to a slow exponential decay. For all systems investigated we found the Onsager distribution function to give by far the best agreement between calculated and experimental scattering patterns.

As the structural parameters of the cylindrical micelles have already been determined in a dilute isotropic solution (Table I), the only adjustable parameter to fit the calculated to the experimental SANS patterns is the orientational order parameter S which is calculated from the distribution of deviation angles $h(\delta)$. Calculated and experimentally determined scattering patterns together with the orientational order parameters S are shown in Fig. 2. Using the Onsager distribution function, the agreement between calculated and experimental scattering curves was excellent until the highest concentration, where a suppression of scattered intensity at low q indicated intermolecular correlations which were taken into account by using a structure factor given by van der Schoot [16].

Using the rheo-SANS data analysis allows one to determine the reduced shear viscosity $\eta_S = \eta - \eta_\infty$ and the orientational order S for a given shear rate $\dot{\gamma}$. Thus, the $\eta(\dot{\gamma})$ curves (Fig. 2) can be converted to the corresponding $\eta_S(S)$ curves. We observe that for nearly all investigated samples and concentrations, the reduced shear viscosity decreases exponentially with increasing order parameter. This is shown in Fig. 3, where the η_S curves have been vertically shifted for superposition by dividing by a factor η_{S0}. Nearly all data sets fall onto a single line in the semilogarithmic presentation. Only PB-PEO-17 at the lowest concentration shows a significantly weaker dependence on the order parameter, whereas PB-PEO-16 and PB-PEO-14 show a stronger dependence at the highest concentration. The concentration dependence of the shift factor η_{S0} for each sample is shown in the inset of Fig. 3.

We observe that solutions of sheared wormlike micelles cover a broad range of order parameters $0.05 \leq S \leq 0.85$ well into the range of order parameters typical for nematic liquid crystals. Over a wide range of concentrations and shear rates we observe a simple exponential behavior of the form $\eta_S = \eta_{S0} e^{-aS}$ with a common slope of $a \approx 13.8$ for

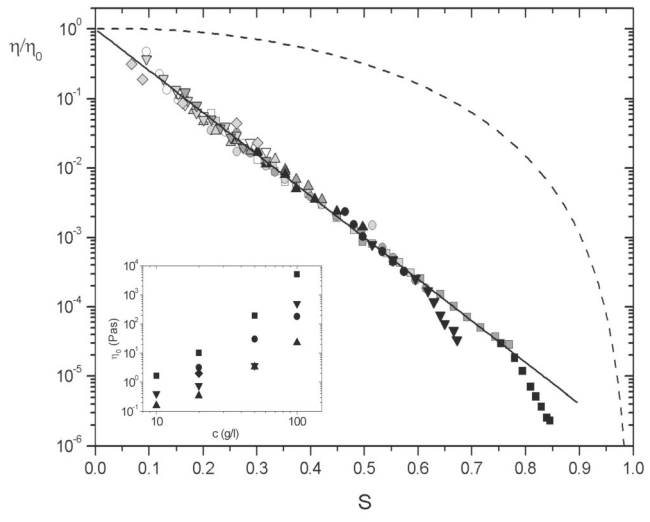

FIG. 3. Dimensionless viscosity η_S/η_{S0} as a function of the orientational order parameter S for all flow curves investigated in the present study: $c = 1\%$ (○), 2% (●), 5% (●), 10% (●) for PB-PEO-14 (▽), PB-PEO-16 (□), PB-PEO-17 (○), GS (△), and CPySal (◆). Nearly all data sets superimpose as indicated by the solid line. The theoretical prediction by Doi and Edwards is shown by the dashed line. The inset shows the shift factors η_{S0} as a function of concentration for all samples.

all samples, except at the highest concentrations where values become significantly larger, i.e., $a \approx 30$. Concentration and micellar thickness enter only the prefactor η_{S0}.

For comparison, Fig. 3 shows the theoretical prediction by Doi and Edwards for rodlike polymers in the nematic phase (Eq. 10.128 of Ref. [5]). The functional form is significantly different, with a weak decrease of the shear viscosity at small order parameters and a strong decrease in the limit $S \rightarrow 1$. The theory considers the shear flow of rodlike molecules determined by the balance of orientational stress and rotational diffusion [2]. As all the samples studied are well above the overlap concentration $c > c*$, the observed deviations may be attributed to the formation of a transient network of entangled micelles, where the balance of orientational stress at a shear rate $\dot{\gamma}$ and the disentanglement time τ_{dis} are the relevant dynamic processes. Disentanglement may occur via breaking or reptation of the micelles. If cylindrical micelles cannot disentangle fast enough at high-shear rates, i.e., for $\tau_{\text{dis}}\dot{\gamma} \gg 1$, the entanglements will propagate stresses in the same manner as chemical cross-links so that the network strands become stretched and oriented. This is consistent with the observation that the shear curves and corresponding shear patterns are completely reversible for shear rate up and down cycles (Fig. 2). Low molecular weight CTAB- and CPySal-cylindrical micelles have considerably shorter disentanglement (breaking) times ($\tau_{\text{dis}} =$ 0.0045 and 0.73 s), and therefore the onset of shear thinning and shear orientation occur at considerably higher shear rates $\dot{\gamma}$. In a study by Hayter and co-workers [3,4] shear rates of $\dot{\gamma} = 5000$–$9000\ \text{s}^{-1}$ had to be used for shear orientation of CTAB solutions. At lower shear rates, cylindrical surfactant micelles show no shear-induced orientation. Block copolymer cylindrical micelles have larger values of τ_{dis}, and therefore shear thinning and orientation are observed already at lower shear rates. We have currently no well-founded explanation for the observed simple $\eta_S = \eta_{S0}e^{-aS}$ behavior. Recent Brownian dynamics simulations of the shear-thinning behavior of dilute polymer solutions show that for high-shear rates $\tau\dot{\gamma} \gg 1$, polymer chains align in shear flow with only small deviations ($<5°$) from the flow direction [17,18]. These studies could be well extended to obtain a quantitative relation between shear viscosity and orientational order parameter.

The observed steeper slopes a for the highest concentrations could be attributed to the presence of nematic domains at high-shear rates. No peaks in the scattering curves indicating the presence of macrophase-separated nematic domains could be detected which could give rise to shear banding, a shear-induced transition to a viscous nematic band, and a lower-viscosity isotropic band at concentrations close to the isotropic-to-nematic transition [19,20].

In summary, this study shows that shear thinning and orientation of wormlike micelles is observed for $\tau_{\text{dis}}\dot{\gamma} \gg 1$, where τ_{dis} is the disentanglement time. In this regime there is a simple $\eta_S = \eta_{S0}e^{-aS}$ relation between shear viscosity and order parameter. Concentration and micellar thickness enter only the prefactor η_{S0}. The study provides direct relations between bulk properties like shear rate and shear viscosity, and molecular properties such as micellar thickness and orientational distribution of long wormlike or fibrous structures. The findings may allow one to better understand and control rheological properties of solutions of chainlike molecules as in flow modifiers and the production of fiber-reinforced materials.

[1] M. E. Cates and J. S. Candau, J. Phys. Condens. Matter **2**, 6869 (1990).
[2] H. G. Jerrard, Chem. Rev. **89**, 345 (1959).
[3] J. B. Hayter and J. Penfold, J. Phys. Chem. **88**, 4589 (1984).
[4] J. Penfold, E. Staples, and P. G. Cummins, Adv. Colloid Interface Sci. **34**, 451 (1991).
[5] M. Doi and E. Edwards, *The Physics of Polymers* (Clarendon Press, Oxford, 1981).
[6] J. F. Berret, D. C. Roux, and P. Lindner, Eur. Phys. J. B **5**, 67 (1998).
[7] H. Thurn, J. Kalus, and H. Hoffmann, J. Chem. Phys. **80**, 3440 (1984).
[8] Y.-Y. Won, H. T. Davis, F. S. Bates, Science **283**, 960 (1999).
[9] S. Förster and E. Krämer, Macromolecules **32**, 2783 (1999).
[10] P. Lindner, in *Neutrons, X-rays and Light: Scattering Methods Applied to Soft Condensed Matter*, edited by P. Lindner and Th. Zemb (Elsevier, Amsterdam, 2002).
[11] R. Koyama, Physica B (Amsterdam) **120**, 418 (1983).
[12] S. Förster and C. Burger, Macromolecules **31**, 879 (1998).
[13] S. Förster, E. Wenz, and P. Lindner, Phys. Rev. Lett. **77**, 95 (1996).
[14] S. Förster, B. Berton, H.-P. Hentze, E. Krämer, M. Antonietti, and P. Lindner, Macromolecules **34**, 4610 (2001).
[15] C. Giacovazzo, in *Fundamentals of Crystallography*, edited by C. Giacovazzo (Oxford University Press, Oxford, 1992).
[16] P. v. d. Schoot, Macromolecules **25**, 2923 (1992).
[17] D. Petera and M. Muthukumar, J. Chem. Phys. **111**, 7614 (1999).
[18] S. Liu, B. Ashok, and M. Muthukumar, Polymer **45**, 1383 (2004).
[19] N. A. Spenley, M. E. Cates, and T. C. B. McLeish, Phys. Rev. Lett. **71**, 939 (1993).
[20] E. Fischer and P. T. Callaghan, Phys. Rev. E **64**, 011501 (2001).